Study of vemurafenib resistance and creating optimal dosing scehdules

Shiv Priyam Raghuraman
School of Mathematics
University of Minnesota, Minneapolis, MN, 55455, USA.

Abstract

Vemurafenib has shown to be very effective in treating late-stage BRAF-mutated melanoma patients. However, the tumor acquires resistance to this drug over time and makes the therapeutic treatment given to the patient ineffective. This paper creates a mathematical model to find optimal dosing schedules under the given toxicity constraints and calculates the probability of acquiring resistance and the population of resistant cells, by analysing the birth, death and growth rates of sensitive and resistant cells.

Introduction

Patients suffering from late-stage melanoma with the BRAF mutated gene are given vemurafenib, a drug successful in tackling this mutation. However, the mutation becomes resistant to the drug during treatment, reducing the drug's efficacy. Resistance to the drug arises due to different mechanisms such as overexpressing a cell surface protein PDGFRB which creates another way for the cancer cells to survive, BRAF survival pathway gets reactivated due to another oncogene NRAS's mutation, and stromal cell secretion of hepatocyte growth factor (HGF). [**?**] [**?**] It was found that resistant tumors showed a continued dependency on $BRAF(V600E) \rightarrow MEK \rightarrow ERK$ signalling owing to related BRAF(V600E) expression. [**?**] An important implication of this is that the vemurafenib resistant cells depended on the drug to continue to reproduce, which meant that a discontinuous dosing schedule would hinder the growth of these resistant cells leading to a hostile environment for the resistant cells.

Quantitatively understanding the manner in which growth and death rates and resistant cell populations are affected by this resistance to the drug, is imperative for creating better treatment schedules and hence can create a better outcome for the patient. By using existing drugs but administering the drug in a manner such that the cancer cells do not become resistant to vemurafenib, the treatment can be extended and hence enhancing chances of remission. If there already exist resistant cells once the treatment has begun, we aim to arrest the growth of these resistant cells.

Since mutations conferring resistance can arise as random events during the DNA replication phase of cell division, the emergence of resistance cells is described well by stochastic mathematical models wherein resistant cells arise during sensitive cell replication. Cells were assumed to divide with a fixed and common interdivision time and each sensitive cell division gives rise to a resistant cell with a certain probability. In this paper, the model assumes the birth and death rate of each cell population is modeled as a general-time dependent function. [**?**] Our model calculates the probability of acquiring resistance to the drug and the number of resistant cells present in the tumor, which are essential indicators of success in a dosing schedule. These factors enabled us to create a model that designs an optimal treatment schedule which minimizes the chance of sensitive cells becoming resistant to the drug, and controls the population of cells already resistant to the drug.

Extraction of birth, death and growth rates

Figure 1 below depicts HMEX1906 mealnomas dose response to vemurafenib for different concentrations.

We assumed that the cell populations grow at an exponential rate. Using Figure 1, we found the growth rates for each concentration. The curve is assumed to be exponentially increasing until it plateaus at 1200 mm^3. Due to its exponential properties we were able to plot a graph of the logarithm of the tumor volume versus time. This is due to the fact that the curve is expressed as $e^{\lambda t}$, where λ is the growth rate of the HMEX1906 cells in response to the drug, and t is the time elapsed measured in days. Then the logarithm of such a curve results in λt as a straight line when plotted against time, and the slope of this straight line would just be the growth rate, λ.

After obtaining the growth rates as described above, we plot in Figure 2 a graph that contains the growth rates versus the concentration. Figure 3b below represents a

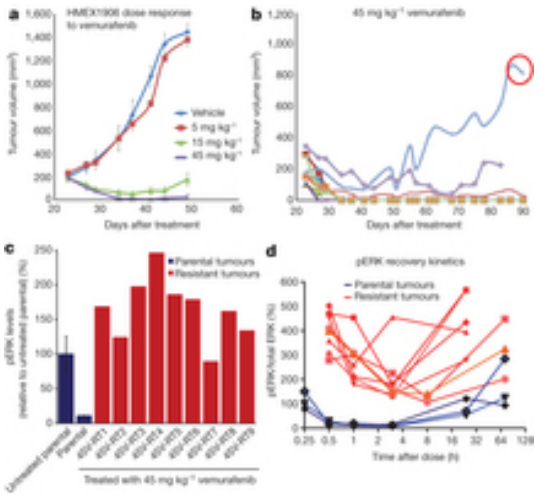

Figure 1: a) Mice bearing subcutaneous HMEX1906 tumors were dosed with vehicle, 5 mg kg^{-1}, 15 mg kg^{-1}, 45 mg kg^{-1} vemurafenib twice daily. [**?**]

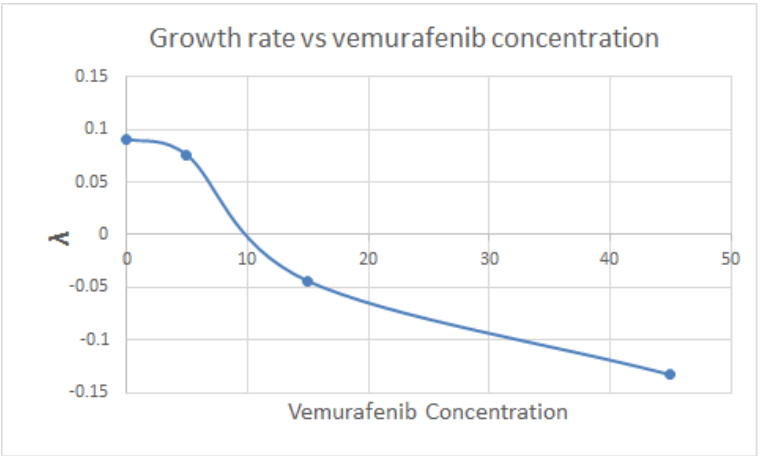

Figure 2: Graph of growth rate vs concentration (mg kg^{-1}) for HMEX 1906 melanoma cells which are sensitive to the drug.

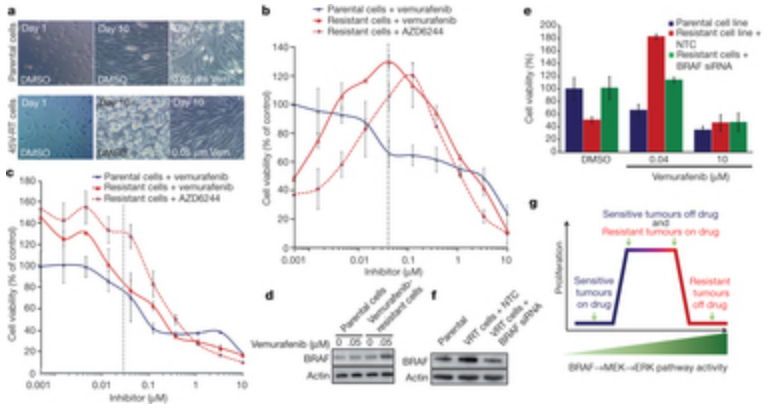

Figure 3: b) Parental and vemurafenib-resistant cells were treated with the indicated concentrations of vemurafenib and AZD6244 for 72 h [**?**]

bell shaped curve. It shows that the resistant cells do not proliferate when there is no drug around and in fact grow faster when the drug is present. We analyzed the data from this and plotted the growth rates of the parental cells and resistant cells versus the concentration of the inhibitor in μM. The growth rate was calculated using the following formula:

$$\lambda = (\text{Cell viability } \%) \cdot \lambda_v \tag{1}$$

where

$$\lambda_v = 0.0911,$$

which is the growth rate of HMEX1906 cells for the vehicle concentration from Figure 2.

Figure 4 contains plots of the growth rates of parental and resistant cells versus concentration. Using the data obtained from this figure, we generated functions relating the growth rate to the concentration for the parental (or sensitive) cells and the resistant cells. The functions are polynomial expressions, which describe the fitted curves. These functions form a core part of the mathematical model designed, which is described in detail in the next section. The growth rate is given by:

$$\lambda = \lambda_b - \lambda_d \tag{2}$$

where λ_b, λ_d are the birth and death rates respectively. We assumed the cell death rate to be a constant and hence the birth rate is just the sum of the growth rate and death rate.

Dosing schedules

The functions relating the growth rates and concentration were used in calculating the probability of acquiring resistance and expected number of resistant cells. To approximate the size of the resistant cell populations, we first estimated the rate at which resistant cells are produced from the sensitive cell population. Then, the expected number of resistant cells was calculated using the following formula [**?**]:

$$R(t) \equiv \int_0^t b(\tau) exp\left[\int_0^{t-\tau} \lambda_Y(\tau+\eta) - \mu_Y(\tau+\eta) d\eta\right] d\tau \tag{3}$$

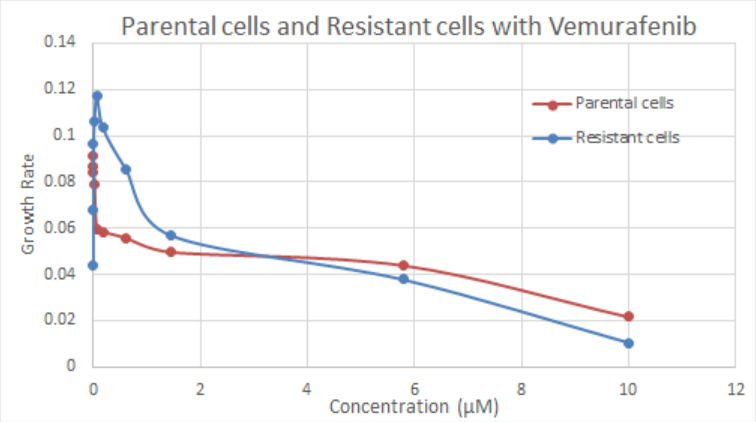

Figure 4: Graph of growth rates of parental and resistant cells versus concentration (μM)

Here, λ_Y is the birth rate of the resistant cell process and μ_Y is the death rate of the resistant cell process and $b(t)$ is the rate of production of resistant cells from the sensitive cell population. To find the probability of resistance we assume that there is at least one resistant cell at a particular time, T. Take N small intervals Δt which make up the time interval $[0, T]$ where $\Delta t = \{t_0, t_1, ..., t_N\}$ and so in general, $t_i = i\Delta t$. The probability of resistance of a mutation arising from the sensitive cell process within a given time interval whose end times are separated only by Δt is $b(t_i)\Delta t$, where $b(t_i)$ is the rate of production of resistant cells from the sensitive cell population as explained before. We assume the population size of a resistant cell clone originating from one resistant cell to be a single-type birth-death process.

This leads us to finding the probability that a clone originating from a single resistant cell produced at time t is extinct by time T. Further, the probability that at time T, there are no resistant cells that have arisen from clones originating in the partition interval $[t_i, t_i + \Delta t]$, is estimated by summing the probability that no sensitive cell divisions give rise to a resistant cell in this interval and the probability that a resistant cell is produced but its clone becomes extinct by time T. Which means that the probability that there are no resistant cells at time T is then the probability that there are no resistant cells at time T that have arisen from clones originating in any partition interval. So, the probability of resistance at time T was calculated using the following formula [**?**]:

$$P_R(T) \equiv 1 - exp\left[\int_0^T -b(t) + b(t)P_{ext}(t, T)dt\right] \tag{4}$$

$P_{ext}(t, T)$ is defined as the probability that a clone originating from a single resistant cell produced at time t is extinct by time T. Further quantitative details about the above qualitatively described quantities can be found in the cited reference.

At the start of treatment if there was a small percentage of resistant cells, we consider the cases of pre-existing resistance. Here, we only consider the case where partial resistance is conferred for otherwise fully resistant cells would be immune to any treatment administered. Under the assumption of partial resistance, we were able to calculate the probability of resistance and expected number of resistant cells using equations (3) and (4). If we consider M as the initial sensitive population size then by including the assumption of pre-existing resistance we have two distinct populations:$M(1 - s)$ sensitive cells and Ms resistant cells, where s is the initial fractions of resistant cells. The probability of resistance and expected of resistant cells are calculated in similar fashion and

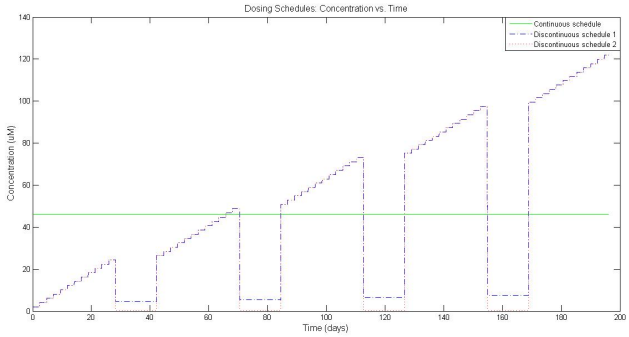

Figure 5: Dosing Schedule

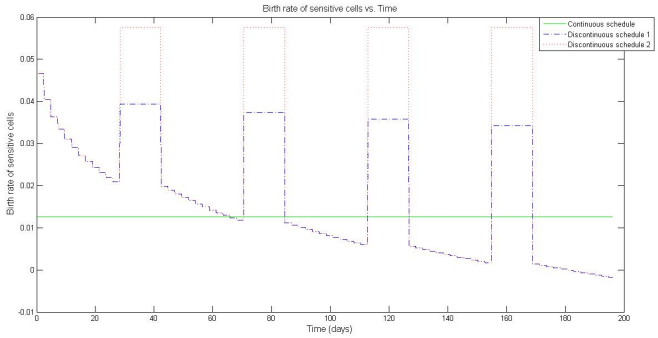

Figure 6: Birth rate of sensitive cells versus time(days)

can be explicitly found in the cited reference. [**?**] Figures 5 through 13 are plots resulting from the model which takes an initial size of one million sensitive cells in the population. The plots are analysed in detail in the next section. The discontinuous and continuous schedules use the same amount of drug and hence a comparison between these schedules reveals the most effective dosing strategy by comparing the values of probability of resistance, expected number of resistant cells and birth rates over the entire treatment cycle. The continuous schedule uses the average dose from the discontinuous schedules but administered without breaks.

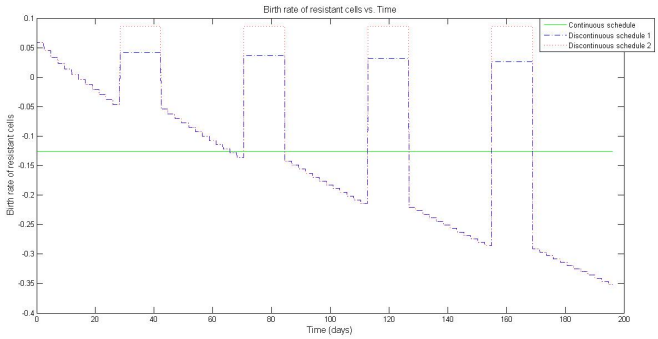

Figure 7: Birth rate of resistant cells versus time(days)

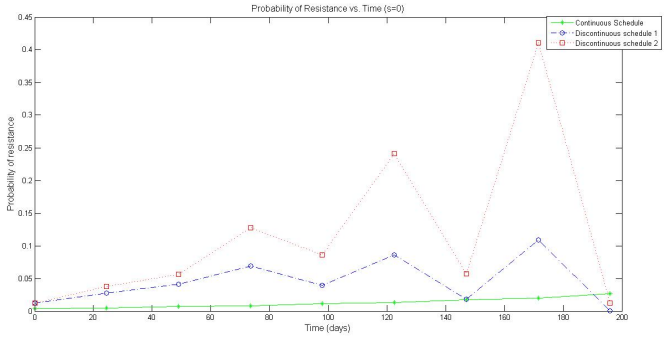

Figure 8: Probaiblity of resistance versus time (s = 0)

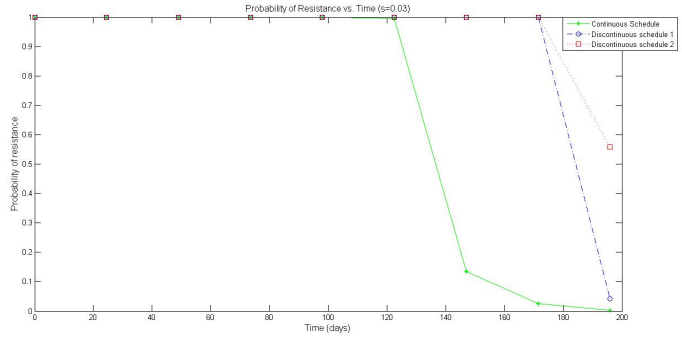

Figure 9: Probaiblity of resistance versus time (s = 0.03)

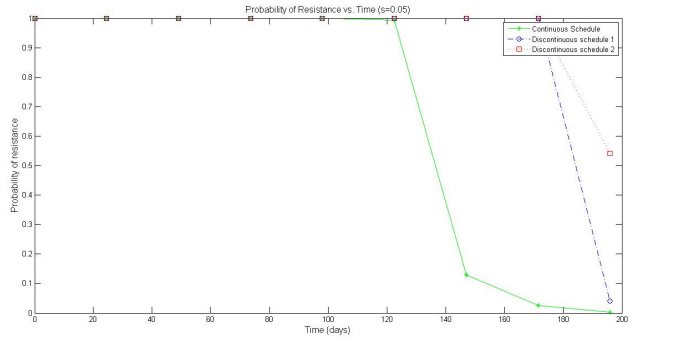

Figure 10: Probaiblity of resistance versus time (s = 0.05)

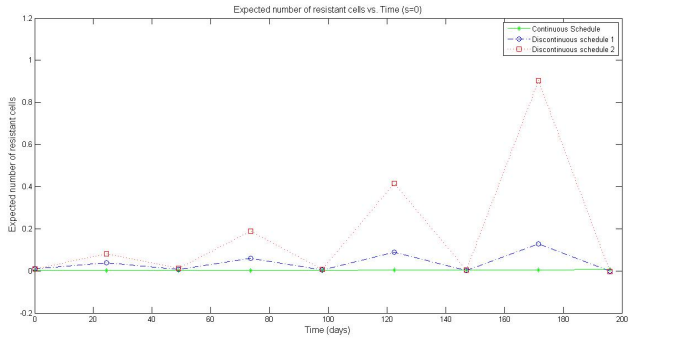

Figure 11: Expected number of resistant cells versus time (s = 0)

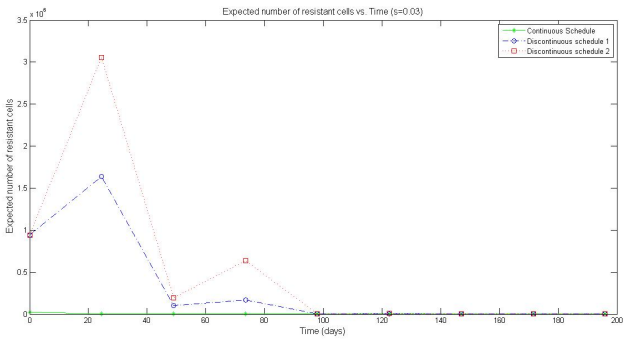

Figure 12: Expected number of resistant cells versus time (s = 0.03)

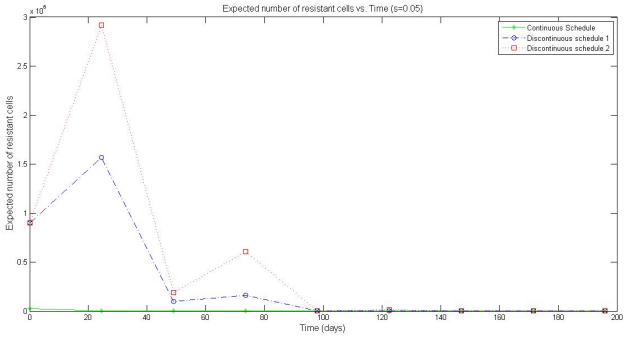

Figure 13: Expected number of resistant cells versus time (s = 0.05)

Discussion

The performance of the discontinuous schedules varies as compared to its counterpart continuous schedules. For example, the birth rate (given by equation (2)) of sensitive cells against time (Figure 6) shows that after half way through the dosing cycle, only the discontinuous schedules show the ability to be at 0 or sub-zero rates. Similarly, the birth rate of resistant cells (Figure 7) after midway through the cycle is very low in the discontinuous schedules as compared to the continuous schedules.

In the probability of resistance cases, the discontinuous schedules in the case of no pre-existing resistance (Figure 8) gets a lower probability at the end of the cycle and the continuous schedule is increasing slowly. What may be causing this behavior is that, during the first few months, a lot of drug is required to tackle the tumor, and the tumor doesn't have the ability to acquire resistance quickly and so the continuous schedule flourishes in the beginning while the discontinuous schedules lag. More precisely, since more than 6 months have passed, the continuous schedule creates an environment for the cancer cells to acquire resistance to the drug which enables the tumor cells to proliferate over the elapsed time period, and hence the probability of resistance increases gradually and towards the end, the probability is higher than its counterparts on the discontinuous schedules. The discontinuous schedules exploit the drug dependency, as seen in Figure 3b, and toward the end of the time period, these schedules display a lower probability of resistance.

In the pre-existing resistance case of s = 0.03 (Figure 9), up to two-thirds of the cycle, all schedules have an equal probability of acquiring resistance equal to 1. This is because if the cell population already has existing resistant cells, it is harder for the

treatment to exterminate them immediately irrespective of the manner in which the dose is administered. Only after 130 days the continuous schedule does better than its counter parts apart from the end where one of the discontinuous schedules catches up after a steep decline in the last 15 days of the cycle. The s = 0.05 plot (Figure 10) is very similar in terms of shape to the previous case but is different in terms of the onset of decrease in probability of resistance in the different schedules.

In the expected number of resistant cells case with no pre-existing resistance (Figure 11), it must be noted that given that there are one million sensitive cells initially and only less than one resistant cell is expected at most for even the worst performing schedule. This can be correlated to the probability of resistance graphs, where the chance of acquiring resistance, or producing resistant cells is minimal in the no pre-existing resistance case. However, the continuous schedule's curve is increasing only slightly over the entire cycle but has a lower number of resistant cells expected throughout. In the pre-existing resistance cases (Figures 12 and 13), the schedules have no distinction between them beyond the first half of the cycle, indicating that the drug can eventually tackle the tumor even if there initially were resistant cells in the population. Initially, when pre-existing resistant cells exist, a large amount of drug is needed to attempt to neutralize these resistant cells and so the continuous schedule achieves that but since the discontinuous schedules give breaks early on, they take almost two months to act effectively.

We notice that the bell shaped curve (Figure 3b) can be exploited towards the end of a discontinuous schedule since the drug begins to become ineffective in large and continuous doses at this point. So, breaking the cycle with rest is imperative at this stage. More investigation could be done to talk about the best practices relating to creating ideal dosing schedules. For example, one could investigate how long can the tumor tolerate continuous dosing of large amounts, and then just before the tumor is predicted to acquire resistance, we switch to a discontinuous schedule which keeps the probability of acquiring resistance at a low, after researching what type of dosing schedule is optimal for a patient who has gone through several months of continuous therapy. One could also study a large range of dose response curves which can be correlated to the key bell shaped resistant response curve, which could give us further quantitative insight into how the tumor cells react to being in the presence of a calculated amount of drug.

Acknowledgements

This research project was conducted under the guidance of Professor Jasmine Foo of the School of Mathematics, University of Minnesota. I would like to thank her for all the help and advice she has provided me with and the patience she exhibited throughout this entire project. This project was funded by Undergraduate Research Opportunities Program (UROP). Many plots and other important parts of the project were done using MATLAB, which I could use due to the license provided by the College of Science and Engineering, University of Minnesota, Twin Cities.

References

[1] Jasmine Foo and Franziska Michor. Evolution of resistance to anti-cancer therapy during general dosing schedules. *Journal of theoretical biology*, 263(2):179–188, 2010.

[2] Ruth Halaban, Wengeng Zhang, Antonella Bacchiocchi, Elaine Cheng, Fabio Parisi, Stephan Ariyan, Michael Krauthammer, James P McCusker, Yuval Kluger, and Mario Sznol. Plx4032, a selective brafv600e kinase inhibitor, activates the erk pathway and enhances cell migration and proliferation of brafwt melanoma cells. *Pigment cell & melanoma research*, 23(2):190–200, 2010.

[3] Ramin Nazarian, Hubing Shi, Qi Wang, Xiangju Kong, Richard C Koya, Hane Lee, Zugen Chen, Mi-Kyung Lee, Narsis Attar, Hooman Sazegar, et al. Melanomas acquire resistance to b-raf (v600e) inhibition by rtk or n-ras upregulation. *Nature*, 468(7326):973–977, 2010.

[4] Meghna Das Thakur, Fernando Salangsang, Allison S Landman, William R Sellers, Nancy K Pryer, Mitchell P Levesque, Reinhard Dummer, Martin McMahon, and Darrin D Stuart. Modelling vemurafenib resistance in melanoma reveals a strategy to forestall drug resistance. *Nature*, 494(7436):251–255, 2013.